CDDpress

www.nature.com/cddis

ARTICLE OPEN

$Ca_v2.2$-NFAT2-USP43 axis promotes invadopodia formation and breast cancer metastasis through cortactin stabilization

Ying Xue[1,2,13], Min Li[1,2,13], Jie Hu[3], Yuanlin Song[3], Wei Guo[4], Changhong Miao[1,5], Di Ge[6], Yingyong Hou[7], Xuefei Wang[8], Xingxu Huang[9], Tianshu Liu[1,10], Xiaoping Zhang[11]✉ and Qihong Huang[1,2,12]✉

© The Author(s) 2022

Distant metastasis is the main cause of mortality in breast cancer patients. Using the breast cancer genomic data from The Cancer Genome Atlas (TCGA), we identified brain specific $Ca_v2.2$ as a critical regulator of metastasis. $Ca_v2.2$ expression is significantly upregulated in breast cancer and its higher expression is inversely correlated with survival suggesting a previously unappreciated role of $Ca_v2.2$ in breast cancer. $Ca_v2.2$ is required for breast cancer migration, invasion, and metastasis. Interestingly, $Ca_v2.2$ promotes invadopodia formation and extracellular matrix (ECM) degradation through the stabilization of invadopodia component cortactin in a proteosome-dependent manner. Moreover, deubiquitinating enzyme USP43 mediated the functions of $Ca_v2.2$ in cortactin stabilization, invadopodia formation, ECM degradation, and metastasis. Interestingly, $Ca_v2.2$ upregulates USP43 expression through NFAT2 dephosphorylation and nuclear localization. Our study uncovered a novel pathway that regulates cortactin expression and invadopodia formation in breast cancer metastasis.

Cell Death and Disease (2022)13:812 ; https://doi.org/10.1038/s41419-022-05174-0

INTRODUCTION

Distant metastasis is the main cause of mortality in breast cancer patients [1]. Patients with metastatic breast cancer generally presents poor prognosis, with an average 5-year survival rate of about 27% [1]. Although surgery, targeted therapy, and radiation therapy have been used to control primary tumor growth, they are not very effective in preventing relapses and in the management of breast cancer metastases. Identification of novel regulators of metastasis may provide potential prognostic markers and therapeutic targets for cancer intervention.

$Ca_v2.2$ belongs to a voltage-dependent calcium channel family, which is required for maintaining Ca^{2+} homeostasis in normal cells [2]. $Ca_v2.2$ is expressed in excitable cells such as neurons, allowing calcium influx after responding to a depolarization of membrane potential [3]. It regulates SNARE-mediated release of neurotransmitters, eventually resulting in synaptic transmission [4]. It is also the main force in supporting transmission of sensory information from nociceptors to spinal cord dorsal horn neurons. Specific inhibition of $Ca_v2.2$ such as ziconotide, an FDA-approved drug, can be used for chronic pain [5–8]. Modulation of $Ca_v2.2$ is involved in synaptic plasticity, synaptogenesis, gene transcription, neuronal survival, and the migration of immature neurons [9, 10]. Moreover, bi-allelic loss-of-function $Ca_v2.2$ variants have been found in progressive epilepsy-dyskinesia, leading to disruption of Ca^{2+} influx and subsequent impaired synaptic neurotransmission [11]. These studies demonstrated that $Ca_v2.2$ plays an irreplaceable role in normal human neural development. However, whether $Ca_v2.2$ is involved in cancer development is largely unknown.

Cancer cells endowed with the ability to degrade extracellular matrix (ECM) can invade surrounding tissues, a crucial step toward in the spreading of the primary tumor and metastasis formation [12, 13]. Notably, invasive cells accomplish this process through invadopodia, a special protruded cell membrane structure with proteolytic activity [14–19]. The protrusive ability of invadopodia is obtained by combining the physical force generated by actin polymerization with the chemical activity of matrix metalloproteinase (MMP)-mediated ECM degradation [20]. A number of signaling pathways including cytoskeletal modulators, adhesive molecules, membrane trafficking regulate invadopodia formation [21, 22]. Actin binding protein cortactin plays an essential role in invadopodia formation [23, 24]. It directly binds to Arp2/3 and N-WASP to promote actin assembly at invadopodia puncta [25–30]. In addition, cortactin regulates ECM degradation through facilitating the secretion of matrix metalloproteinases [24, 27, 31]. It has been shown that cortactin can be regulated by phosphorylation and acetylation [32–36]. However, it has not been studied whether deubiquitination process can regulate cortactin and its functions in invadopodia formation.

[1]Cancer Center, Zhongshan Hospital, Fudan University, Shanghai, PR China. [2]Institute of Clinical Sciences, Zhongshan Hospital, Fudan University, Shanghai, PR China. [3]Department of Pulmonary and Critical Care Medicine, Zhongshan Hospital, Fudan University, Shanghai, PR China. [4]Department of Laboratory Medicine, Zhongshan Hospital, Fudan University, Shanghai, PR China. [5]Department of Anesthesiology, Zhongshan Hospital, Fudan University, Shanghai, PR China. [6]Department of Thoracic Surgery, Zhongshan Hospital, Fudan University, Shanghai, PR China. [7]Department of Pathology, Zhongshan Hospital, Fudan University, Shanghai, PR China. [8]Department of General Surgery/Gastric Cancer Center, Zhongshan Hospital, Fudan University, Shanghai, PR China. [9]School of Life Science and Technology, ShanghaiTech University, Shanghai, PR China. [10]Department of Medicial Oncology, Zhongshan Hospital, Fudan University, Shanghai, PR China. [11]The Institute of Intervention Vessel, Tongji University School of Medicine, Shanghai, PR China. [12]Shanghai Respiratory Research Institute, Shanghai, PR China. [13]These authors contributed equally: Ying Xue, Min Li. ✉email: zxpsibs@163.com; qihong_huang@fudan.edu.cn

Edited by: Nickolai Barlev

Received: 8 February 2022 Revised: 3 August 2022 Accepted: 9 August 2022
Published online: 22 September 2022

Using bioinformatic analysis of TGCA data of breast cancer, we discovered that high $Ca_v2.2$ expression was inversely correlated with breast cancer overall survival, especially in triple negative breast cancer patients. We showed that $Ca_v2.2$ expression was upregulated in breast cancer tissues and cell lines but was absent in normal breast epithelial cells as well as normal breast tissues. We demonstrated that $Ca_v2.2$ was required for breast cancer migration, invasion, and metastasis. Mechanistically we showed that $Ca_v2.2$ promoted invadopodia formation and focal matrix degradation. Conversely, knockdown of $Ca_v2.2$ expression suppressed invadopodia formation and ECM degradation. In addition, we showed that deubiquitinating enzyme USP43 stabilized cortactin and mediated the functions of $Ca_v2.2$ in invadopodia formation and metastasis in breast cancer. Taken together, we discovered a novel pathway that $Ca_v2.2$ regulated invadopodia formation through deubiquitination process.

MATERIALS AND METHODS

Cell culture, plasmids and antibodies

MDA-MB-231, MDA-MB-436, BT-549 were purchased from Cell Bank of the Chinese Academy of Sciences (Shanghai, China). All cell lines were maintained at 37 °C in RPMI 1640 medium supplemented with 10% fetal bovine serum (FBS), 100 IU/ml penicillin and 100 μg/ml streptomycin.

$Ca_v2.2$ plasmid was purchased from Addgene (Plasmid: #62574). Full length of USP43 and Cortactin were amplified by PCR and cloned into Flag-HA-Phase vector and Flag-pcDNA3.1 vector. Full length of NFAT2 was amplified by PCR and cloned into PCDH vector.

Anti-$Ca_v2.2$ was purchased from Proteintech, and antibodies against Cortactin, USP43, NFAT2, p-NFAT2 were purchased from Abcam. Anti-ubiquitin was purchased from Santa Cruze. Antibodies against Flag, IgG, NFAT3 were purchased from Cell signaling.

Transfection and virus production

For transient transfection, cells were transfected with Lipofectamine 2000 according to manufacturer's procedure. Briefly, cells were seeded 24 h prior to transfection. The plasmid(s) of interest and Lipofectamine reagent were mixed in Opti-MEM media. Media was then replaced with regular media without antibiotics 6 h post-transfection. Control shRNA, $Ca_v2.2$ shRNA, USP43 shRNA, NFAT2 shRNA, cortactin cDNA or vector along with the packaging plasmids PMD2.G and PSPAX were transfected using Lipofectamine 2000 (Invitrogen) to produce lentivirus as previously described [37]. Infectious lentiviruses were collected 24 h and 48 h after transfection, centrifuged to remove cell debris and filtered through 0.22 mm filters (Millipore).

CCK8 (Cell counting kit) assay

Cells were seeded in 96-well plates for 24 hours (h), 48 h, 72 h, 96 h. Culture medium was removed, then fresh medium was added to each well along with 10 μl of CKK8 solution (Takara). The absorbance was measured at a wavelength of 450 nm after incubation at 37 °C for 4 h.

Cell counting assay

Cell number was determined using a Hemocytometer. Briefly, 50000 cells were seeded in 12-well plates for 24 h, 48 h, 72 h, 96 h, washed with PBS, digested with trypsin followed by adding supplemented DMEM and mixing cells by pipetting until cells formed a single cell suspension. Hemocytometer was used to determine cell number.

Transwell migration and invasion assay

In vitro cell migration and invasion assays were performed as described previously [38]. Briefly, Cells were incubated in serum-free medium for 24 h, and then were collected, counted, suspended in serum-free medium. Cell suspension were seeded in the upper chamber containing 200 ml serum-free medium with an uncoated or Matrigel-coated membrane, while 600 ml RPMI1640 medium with 10% FBS was added into the lower chamber. After cultured for 48 h, cells were fixed using 4% methyl alcohol for 15 min following staining via 5% crystal violet solution for additional 15 min. Five fields of view were randomly selected and photographed using an upright Metallurgical Microscope (Olympus, Japan).

Quantification of $Ca_v2.2$ expression in human tissues

Total RNAs of normal human tissues were purchased from Clontech and cDNA was synthesized from total RNA using Reverse Transcription Kit (Takara) according to the manufacturer's instructions. Quantitative real-time PCR was carried out by QuantiTect SYBR Green PCR Kit (Takara). The average of three independent analyses was used.

Quantitative real-time PCR

Total RNAs were extracted from cells at utilizing Trizol reagent (Takara) and reverse transcribed with cDNA Reverse Transcription Kit (Takara) according to the manufacturer's instructions. Quantitative real-time PCR was performed by QuantiTect SYBR Green PCR Kit (Takara) using an Applied Biosystems Q5 Real-time PCR system. Relative mRNA expressions were determined by 2−delta delta (Ct-Cc) where Ct and Cc are the mean threshold cycle differences after normalizing to beta-actin values.

Tumor transplantation in mice

In vivo tumor transplantation assay was performed as described previously [38]. The MDA-MB-436 human breast cancer cell lines stably expressing Firelfly Luciferase gene with $Ca_v2.2$ shRNA or control shRNA were suspended in 100 μl of PBS and injected in the lateral tail vein of 6–8 weeks old female NOD/SCID mice. Then, IVIS 200 Imaging system (Xenogen Corporation, Hopkinton, MA) was used to image mice bearing luciferase positive tumors. The primary tumors and lung metastasis were analyzed using bioluminescent flux (photons per second per steradian per centimeter square). In order to minimize the number of animals we used power analysis to calculate the minimum sample size using the free software DOEUMH (https://samplesizeumh.shinyapps.io/DOEUMH) based on the TrialSize library of the R program (R Core Team). We selected the procedure KMeans – ANOVA, fixing the significance to 0.05, power to 0.08, and a drop-out of 5%. We took into consideration differences between averages of about 1.5–2 fold. Minimum number of mice/group: 5–6 mice/group. Animal experiment protocols were approved by the Institutional Animal Care and Use Committee (IACUC) of the Zhongshan Hospital. Animal procedures were conducted in compliance with the IACUC.

Invadopodia formation assay

Sterile coverslips were incubated in 0.1 mg/ml poly-D-lysine for 10 minutes at room temperature followed by incubating 2% gelatin (Sigma) for 1 h at 37 °C. Then, coverslips were added 0.25% gluteraldehyde/PBS for 15 min followed by PBS wash three times. Coverslips were then incubated for 15 min in 5 mg/ml $NaBH_4$ followed by PBS wash three times. The coverslips were then incubated at 37 °C in 10% calf serum/RPMI1640 for 2 h. Cells were seeded on each coverslip and incubated for 8 h, and fixed at 37 °C in 4% paraformaldehyde (PFA)/PBS for 15 min, permeabilized with 0.1% Triton X-100/PBS for 10 min, and blocked with 3% goat serum. Samples were incubated with primary antibodies overnight at 4 °C and with secondary antibodies and/or phalloidin for 2 h. Images were taken using Olympus BX43F microscope. Co-localization of cortactin (green) and F-actin(red) puncta was used to identify invadopodia.

Focal ECM degradation assay

Oregon Green™ gelatin 488 (Invitrogen) was used for focal gelatin degradation assay. Briefly, sterile coverslips were coated with a mix of 0.1 mg ml^{-1} poly-d-lysine followed by incubation with 0.4% glutaraldehyde for 20 min and PBS wash three times. Oregon Green™ gelatin 488 was diluted 1:50 with 0.1% unconjugated gelatin and used to coat coverslips at 37 °C for 1 h. Coverslips were then incubated with 5 mg/ml $NaBH_4$ for 1 min, followed by 70% ethanol for 20 min. Three washes with 1 × PBS were performed between each step. RPMI1640 media was added to the coverslips at 37 °C for 1 h before cell plating. The coverslips were then incubated at 37 °C in 10% calf serum/RPMI1640 for 2 h. Cells were seeded on each coverslip, incubated for 8 h, fixed at 37 °C in 4% paraformaldehyde (PFA)/PBS treated for 15 min, and permeabilized with 0.1% Triton X-100/PBS for 10 min. F-actin/Phalloidin (1:1,000; Cat. #: A22287, ThermoFisher Scientific) was used to incubate the coverslips for one hour. DAPI (Cat. #: D3571, Invitrogen) was used to visualize nuclei. Images were taken using Olympus BX43F microscope. Gelatin degradation was quantified using ImageJ software. To measure the percentage of degraded area in each field, identical signal threshold for the Oregon Green -gelatin fluorescence is set for all images and the degraded area with Oregon Green signal

below the set threshold was measured by ImageJ. The resulting percentage of degradation area was further normalized to total number of cells (counted by DAPI staining for nuclei) in each field. The final gel degradation index is the average percentage degradation per cell obtained from fields.

Protein stability assay
To examine cortactin protein turnover, cycloheximide (0.1 mg/ml) was added to cell culture medium and cells were harvested at the indicated time points. Cells were then lysed in RIPA lysis buffer and cell lysates were subjected to Western blot with anti-cortactin, anti-USP43, or anti-$Ca_v2.2$ and anti-β-actin as indicated.

In vivo deubiquitination assay
MDA-MB-231 cells were treated with MG132 for 6 h before harvesting. The cells were lysed in 800 µl IP-lysis buffer containing protease inhibitors, 20 mM NEM, and 1 mM iodoacetamide, centrifuged to remove cell debris. The cell extracts were subjected to immunoprecipitation with Flag-beads at 4 °C. After washing with IP lysis buffer (containing 20 mM NEM and 1 mM iodoacetamide) four times, the immunocomplexes were separated by SDS–PAGE and blotted with anti-Ub antibody.

Co-immunoprecipitation (co-IP) assay
Cells were harvested and washed by PBS before lysed with IP lysis buffer (Meilunbio, China) with 1 mM PMSF. Whole cell lysates obtained by centrifugation were incubated with 2 µg of anti-Flag-beads (sigma) at 4 °C. After washing with IP lysis buffer three times, the immunocomplexes were separated by SDS–PAGE. Immunoblotting was performed following standard procedures.

Measurement of intracellular calcium
Cells were loaded with calcium-sensitive fluorescent dye 1 µM Fura-2AM (Beyotime) for 40 min at room temperature in the dark and then washed three times in standard external solution of 145 mM NaCl, 2.8 mM KCl, 2 mM $CaCl_2$, 2 mM $MgCl_2$, 10 mM D- glucose, 10 mM HEPES, pH 7.4, with NaOH. Fluorescence was measured with fluorescence spectrophotometer by varioskan LUX (Thermo Fisher Scientific), where excitation was performed at 340 nm and 380 nm. The fluorescence intensity (F340/F380) indicated an intracellular calcium concentration.

Dual luciferase reporter assay
USP43 promoter was cloned into pGL3 basic plasmid to construct pGL3-USP43 promoter-Luc plasmid. MDA-MB-231 cells were cultured in 12-well plates. MDA-MB-231 cells expressing control vector or NFAT2 were co-transfected 500 ng USP43 promoter-Luc plasmid and 20 ng Renilla using lipofectamine 2000 (Invitrogen). Firefly and Renilla luciferase activities were measured using the dual-luciferase reporter assay system 48 h after transfection (Cat:#E1910, Promega).

Chromatin immunoprecipitation (ChIP)
ChIP were performed according to manufacture's protocol (Cat:#53040,-Active motif). Briefly, two 10 cm dishes MDA-MB-231 cells were cross-linked and lysed. Cells were sonicated using the Bioruptor Pico (Diagenode) for 30 s on/30 s off for 15 cycles. Chromatin was immunoprecipitated with the specific antibody at 4 °C overnight, followed by incubation with protein A/G beads for 3 h at 4 °C. The immune complex was then eluted from beads and was reversed cross-linked by incubating in elution buffer. The DNA fragments were purified and used for qPCR using SYBR Green Master Mix.

Immunofluorescence staining
Cells were plated on the glass slides in 12-wells. Then cells were fixed with 4% paraformaldehyde for 15 min at room temperature. After being washed twice with PBS, the cells were permeabilized with 0.1% Triton-X100 for 30 min and blocked with 5% BSA for 1 h at room temperature. Cells were incubated with a primary antibody against NFAT2 at the ratio of 1:300 at 4 °C overnight, and subsequently incubated with a secondary antibody at room temperature for 1 h, followed by mounting with Vectashield Mounting Media with DAPI (H-1200, Vector Laboratories). Images were taken using Olympus BX43F microscope and analyzed with ImageJ.

RESULTS
Identification of $Ca_v2.2$ in breast cancer progression
To identify critical genes that drive breast cancer progression, we analyzed The Cancer Genome Atlas (TCGA) RNA-seq data of breast cancer and normal breast tissues and the relevant survival data of breast cancer patients [38]. From the analysis, 41 genes were identified that met the four inclusion criteria as described previously [38]. In this study, we focused on the calcium channel $Ca_v2.2$ because (1) very little is known about its functions in cancer development; (2) it is expressed in breast cancer but not in normal tissues other than brain; (3) it is a cell surface protein which can be targeted by small molecule compounds or antibodies; (4) FDA-approved therapeutics targeting $Ca_v2.2$ is already used in clinics for chronic pain. We first determined the $Ca_v2.2$ expression in a panel of normal human tissues and found that it is exclusively expressed in adult and fetal brain tissues (Fig. 1A). Interestingly, $Ca_v2.2$ expression was upregulated in breast cancer tissues than adjacent normal breast tissues (Fig. 1B). In particular, $Ca_v2.2$ expression was significantly upregulated in triple negative breast cancer (TNBC) (Fig. 1C), which has worse prognosis than other subtypes in breast cancer. Consistent with the $Ca_v2.2$ expression in breast cancer tissues, $Ca_v2.2$ was expressed at various levels in breast cancer cell lines but not in human normal breast epithelial cell line HMEL (Supplementary Fig. 1). In paired human breast cancer samples, $Ca_v2.2$ expression was significantly higher in the metastatic samples than in the matched primary breast cancer samples (Fig. 1D). We further investigated the correlation of $Ca_v2.2$ expression with survival. Patients with higher $Ca_v2.2$ expression had worse overall survival than those with lower $Ca_v2.2$ expression in breast cancer (Fig. 1E) and the TNBC subtype (Fig. 1F). Taken together, these data indicated that $Ca_v2.2$ expression is up-regulated in breast cancer and a potential prognosis marker for survival.

$Ca_v2.2$ is required for breast cancer invasion and metastasis
As $Ca_v2.2$ appeared to have higher expression in metastatic tissues than in primary tumors and metastasis is a major factor in patient survival, we assessed the role of $Ca_v2.2$ in breast cancer invasion and metastasis. We introduced $Ca_v2.2$ into human breast cancer cell BT549 which expresses endogenous $Ca_v2.2$ at a very low level. The expression of $Ca_v2.2$ in BT549 was confirmed by real-time PCR (Supplementary Fig. 2). The cells were subjected to transwell assays. $Ca_v2.2$ significantly increased cell migration and invasion (Fig. 2A, B) without affecting cell proliferation (Supplementary Fig. 3). To investigate whether $Ca_v2.2$ is required for migration and invasion, we introduced short hairpin RNA constructs into human breast cancer cell lines MDA-MB-231 and MDA-MB-436. Knock-down of $Ca_v2.2$ expression was confirmed by real-time PCR (Supplementary Figs. 4 and 5). $Ca_v2.2$ knock-down significantly reduced cell migration and invasion in MDA-MB-231 and MDA-MB-436 (Fig. 2C–F) without affecting cell growth (Supplementary Fig. 6, Supplementary Fig. 7). To investigate the function of $Ca_v2.2$ in metastasis, we knocked down $Ca_v2.2$ in luciferase-tagged MDA-MB-436 cells and transplanted these cells into mice. Nine out of ten mice transplanted with cells expressing a control shRNA construct developed metastasis (Fig. 2G), only two out of ten mice transplanted with cells expressing $Ca_v2.2$ shRNA developed metastasis (Fig. 2G). The luciferase signal of metastasis was also much higher in these nine mice (Fig. 2G). These results indicated that $Ca_v2.2$ was required for cell migration, invasion, and metastasis.

$Ca_v2.2$ promotes invadopodia formation and extracellular matrix degradation
The invasiveness of cancer cells depends on their ability to degrade extracellular matrix (ECM) and invade into neighboring tissues as well as lymph node and bloodstream [12, 39]. Their invasiveness is decided by special cell membrane structure

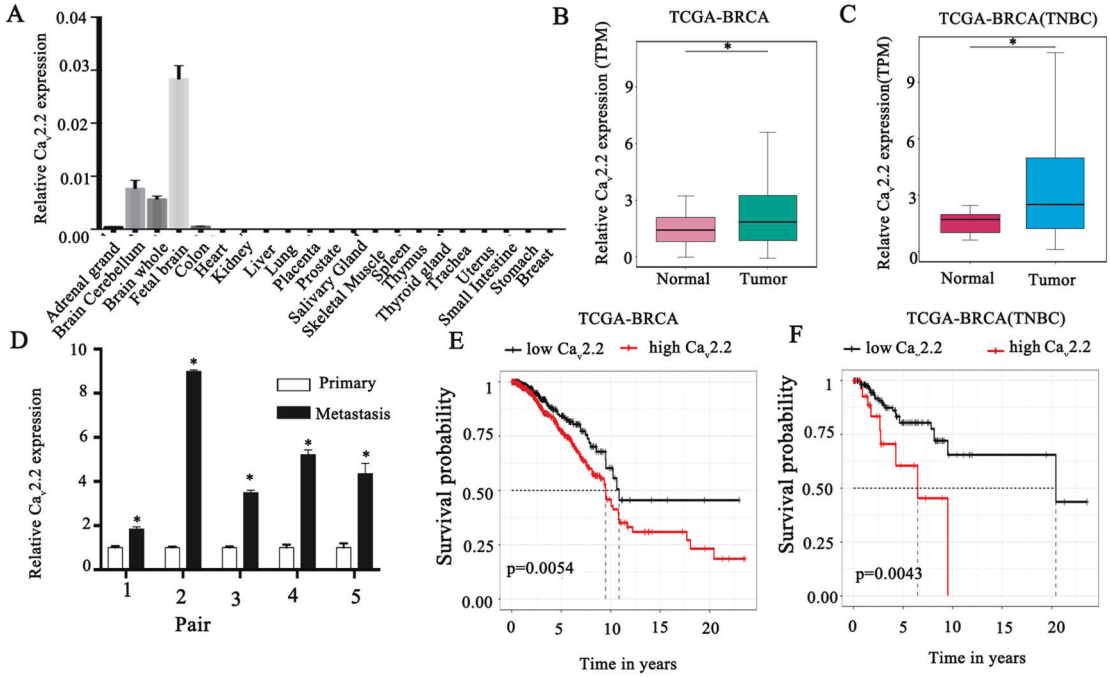

Fig. 1 Cav2.2 is expressed in human breast cancer tissues but not in normal human breast tissues. A Expression of $Ca_v2.2$ transcript in normal human tissues. Error bars represent mean ± sd **B** Expression of Cav2.2 transcript in breast cancer tissues and normal tissues. *$p < 0.05$. **C** Expression of Cav2.2 transcript in triple negative breast cancer (TNBC) tissues and adjacent normal tissues. *$p < 0.05$. **D** Expression of Cav2.2 transcript in paired metastatic and primary human breast cancer tissues. *$p < 0.02$. **E** Association of higher Cav2.2 expression with poor survival in breast cancer (Cox regression $P = 0.0054$, hazard ratio = 1.58). **F** Association of higher Cav2.2 expression with poor survival in triple negative breast cancer (Cox regression $P = 0.0043$, hazard ratio = 2.95).

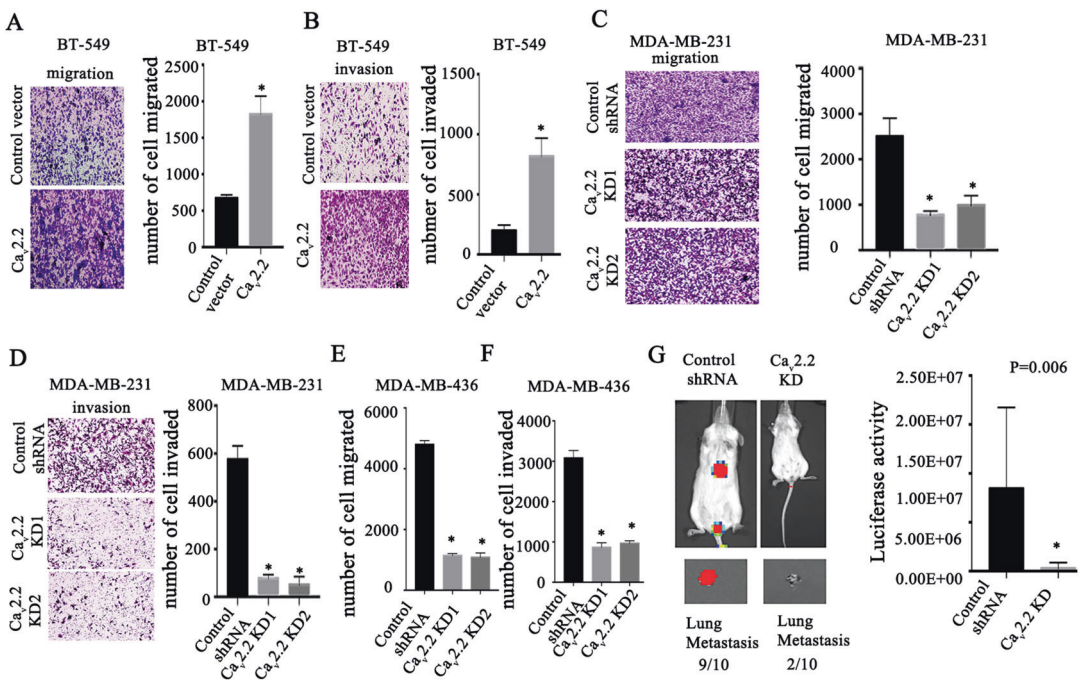

Fig. 2 Cav2.2 is required for migration, invasion and metastasis in breast cancer. Human breast cancer BT-549 cells transfected with Cav2.2 cDNA or a control vector were subjected to migration **A** and invasion **B** assays. Representative images of migrated or invaded cells were shown. The numbers of migrated and invaded cells were quantified. P value was determined using Student's t-test (*$p < 0.001$). Error bars represent mean ± s.d. Human breast cancer MDA-MB-231 cells stably expressing Cav2.2 shRNA or control shRNA were subjected to migration **C** and invasion **D** assays. Representative images of migrated or invaded cells were shown. The numbers of migrated and invaded cells were quantified. *P* value was determined using Student's t-test (*$p < 0.001$). Error bars represent mean ± sd. Human breast cancer MDA-MB-436 cells stably expressing Cav2.2 shRNA or control shRNA were subjected to migration **E** and invasion **F** assays. The numbers of migrated and invaded cells were quantified. *P* value was determined using Student's t-test (*$p < 0.001$). Error bars represent mean ± sd. **G** Luciferase-tagged human breast cancer MDA-MB-436 cells stably expressing Cav2.2 shRNA or control shRNA were transplanted in mice. Metastasis were imaged using Xenogen bioluminescence system. *P* value was determined using Fisher's exact test ($p = 0.006$).

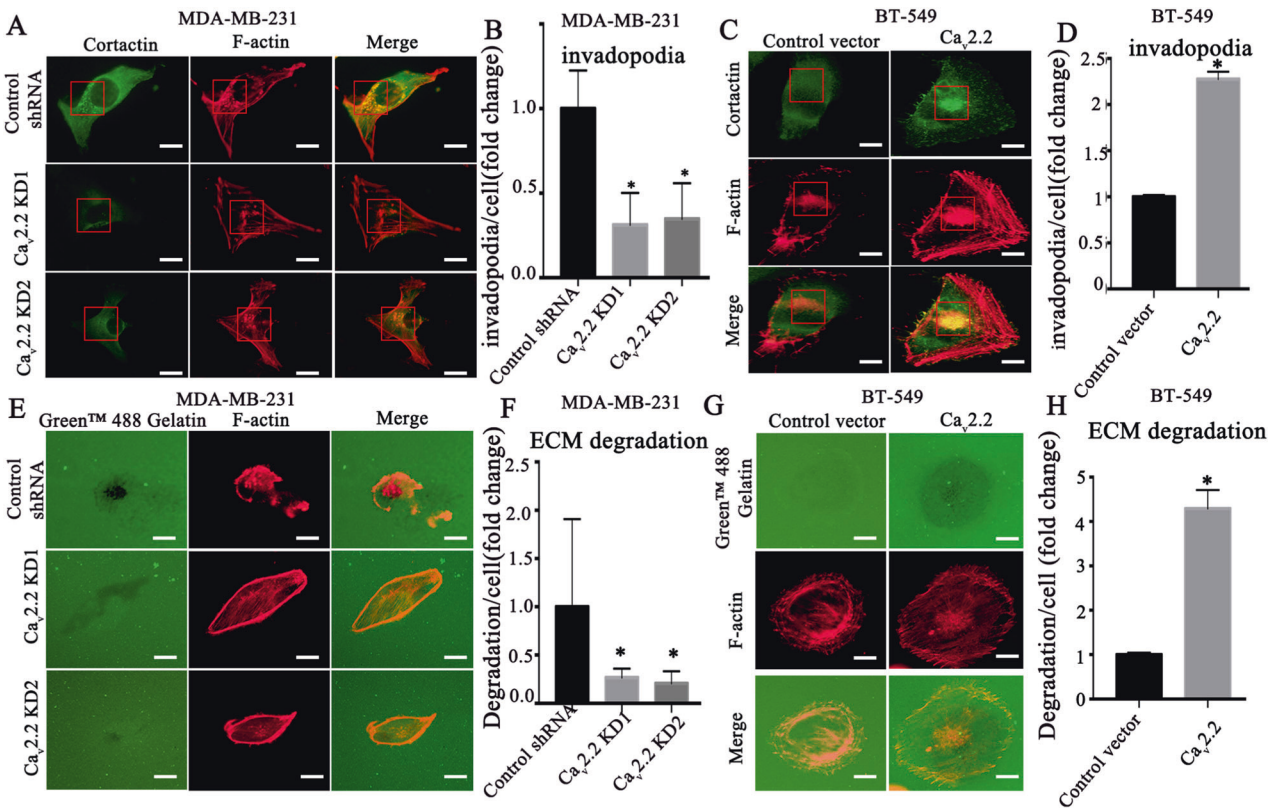

Fig. 3 Cav2.2 promotes invadopodia formation and ECM degradation. **A** Human breast cancer MDA-MB-231 cells stably expressing $Ca_v2.2$ shRNA or control shRNA were subjected to invadopodia formation assay. Invadopodia were visualized by co-localization of cortactin (green) and F-actin puncta (red). Representative images were shown. Bars: 5 μm. **B** Quantification of invadopodia in MDA-MB-231 cells. *P* value was determined using Student's t-test (*$p < 0.01$). Error bars represent mean ± s.d. **C** Human breast cancer BT-549 cells transfected with $Ca_v2.2$ cDNA or a control vector were subjected to invadopodia formation assay. Invadopodia were visualized by co-localization of cortactin (green) and F-actin puncta (red). Representative images were shown. Bars: 5 μm. **D** Quantification of invadopodia in BT-549 cells. *P* value was determined using Student's t-test (*$p < 0.01$). Error bars represent mean ± sd. **E** MDA-MB-231 cells stably expressing $Ca_v2.2$ shRNAs or control shRNA were subjected to ECM degradation assay. Focal matrix degradation was defined by co-localization of F-actin and degradation regions. Representative images were shown. Bars: 5 μm. **F** Quantification of ECM degradation in MDA-MB-231 cells. P value was determined using Student's t-test (*$p < 0.01$). Error bars represent mean ± $^{s.d.}$ **G** BT-549 cells transfected with $Ca_v2.2$ cDNA or a control vector were subjected to ECM degradation assay. Focal matrix degradation was defined by co-localization of F-actin and degradation regions. Representative images were shown. Bars: 5 μm. **H** Quantification of ECM degradation in BT-549 cells. *P* value was determined using Student's t-test (*$p < 0.01$). Error bars represent mean ± sd.

invadopodia which are dynamic actin-enriched cell protrusions with proteolytic activity. Co-localization of F-actin with the actin-bundling protein cortactin can be used to identify invadopodia [40]. To dissect the cellular functions of $Ca_v2.2$ in invadopodia formation, $Ca_v2.2$ knock-down or over-expression cells were plated on gelatin matrix and labeled for F-actin and cortactin. We found that knock-down of $Ca_v2.2$ potently suppressed the ability of MDA-MB-231 cells to form invadopodia (Fig. 3A, B). Conversely, $Ca_v2.2$ overexpression significantly increased invadopodia formation in BT-549 cells (Fig. 3C, D). Interestingly, immunofluorescence also showed that Cav2.2 knock-down significantly decreased fluorescence intensity of cortactin (Supplementary Fig. 8A), whereas $Ca_v2.2$ overexpression significantly increased cortactin fluorescence intensity (Supplementary Fig. 8B). These results suggested that $Ca_v2.2$ modulates cortactin protein expression. Since functional invadopodia are able to degrade localized ECM, we determined whether $Ca_v2.2$ was required to accelerate focal matrix degradation by gelatin degradation assay. Indeed, $Ca_v2.2$ knock-down cells showed a significantly reduced capability to degrade focal ECM (Fig. 3E, F). Conversely, expression of $Ca_v2.2$ led to dramatically increased degradation of focal ECM (Fig. 3G, H). Taken together, these data demonstrated that $Ca_v2.2$ is sufficient and required for invadopodia formation and ECM degradation.

$Ca_v2.2$ stabilizes cortactin in a proteosome-dependent manner

To gain insight into the underlying mechanism of $Ca_v2.2$ in the regulation of invadopodia formation, we examined whether $Ca_v2.2$ regulated the cortactin expression given that cortactin plays a key role in the formation of invadopodia and invadopodia associated ECM degradation [41–43] and our immunofluorescence analysis showed $Ca_v2.2$ regulated cortactin expression. Immunoblotting analysis showed that the cortactin protein expression was greatly decreased after $Ca_v2.2$ knock-down in MDA-MB-231 cells (Fig. 4A), whereas the cortactin transcript was not changed in $Ca_v2.2$ knock-down cells (Fig. 4B). Conversely, expression of $Ca_v2.2$ in BT-549 cells resulted in a significant increase of cortactin protein expression (Fig. 4A), but not cortactin transcript (Fig. 4C). These results suggested a mechanism involving post-transcriptional regulation of cortactin. Ubiquitination and deubiquitination are among the most widely-used protein modifications in regulating cellular signaling and homeostasis [44]. Because ubiquitination generally modulates target expression by inducing proteasome-dependent degradation [45], we added the proteasome inhibitor MG132 into MDA-MB-231 cells expressing $Ca_v2.2$ shRNA or control shRNA. We found that the decrease in cortactin expression by $Ca_v2.2$ knock-down could be reversed by the addition of MG132, suggesting that $Ca_v2.2$ regulates cortactin in a proteasome-

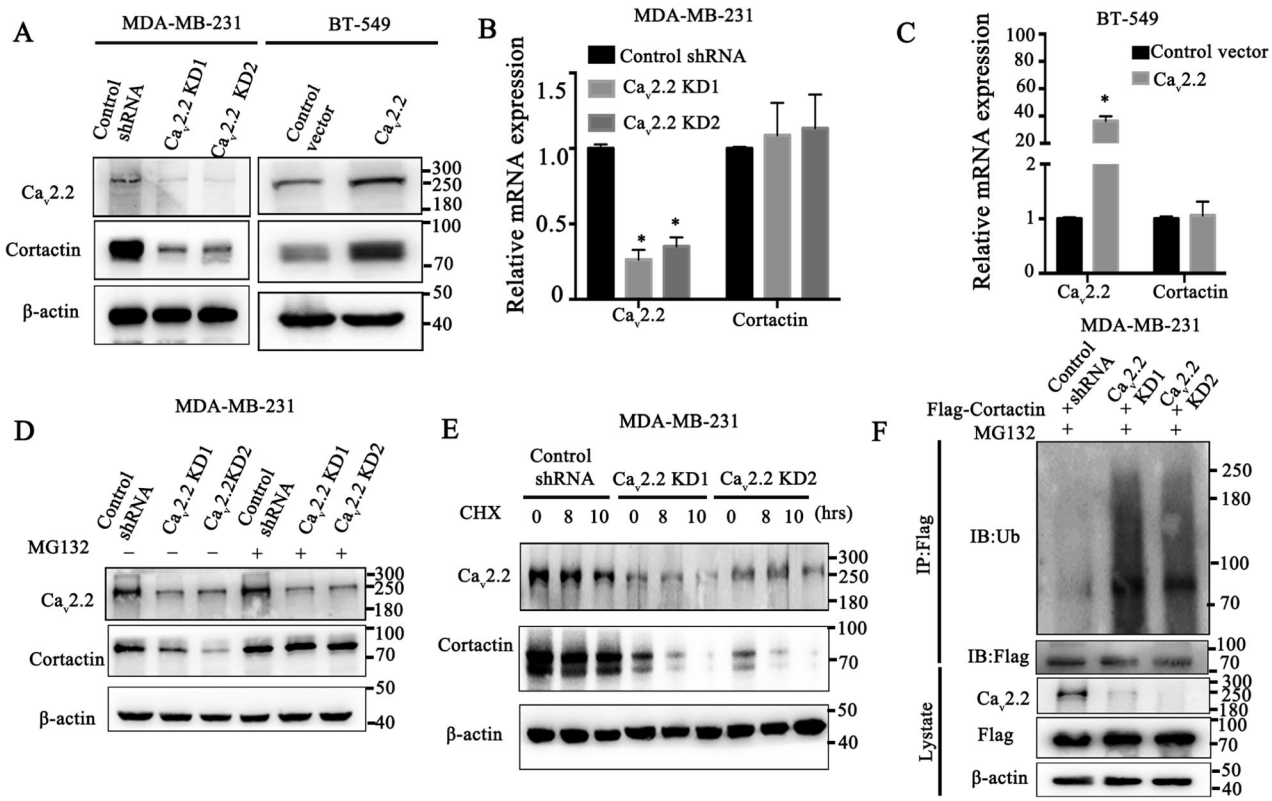

Fig. 4 Cav2.2 stabilizes cortactin in a proteosome-dependent manner. A $Ca_v2.2$ and cortactin were determined by immunoblotting in MDA-MB-231 cells stably expressing $Ca_v2.2$ shRNA or control shRNA and BT-549 cells transfected with $Ca_v2.2$ cDNA or a control vector. **B** $Ca_v2.2$ and cortactin transcripts were determined by qRT-PCR in MDA-MB-231 cells stably expressing $Ca_v2.2$ shRNA or control shRNA. P value was determined using Student's t-test (*$p < 0.001$). Error bars represent mean ± s.d. **C** $Ca_v2.2$ and cortactin transcripts were determined by qRT-PCR in BT-549 cells transfected with $Ca_v2.2$ cDNA or control vector. P value was determined using Student's t-test (*$p < 0.001$). Error bars represent mean ± s.d. **D** $Ca_v2.2$ and cortactin were determined by immunoblotting in MDA-MB-231 cells stably expressing $Ca_v2.2$ shRNA or control shRNA and treated with proteasome inhibitor MG132 or a control vehicle. **E** $Ca_v2.2$ and cortactin were determined by immunoblotting in MDA-MB-231 cells stably expressing $Ca_v2.2$ shRNA or control shRNA and treated with protein synthesis inhibitor cycloheximide (CHX) or a control vehicle. **F** MDA-MB-231 cells stably expressing Flag-tagged cortactin and $Ca_v2.2$ shRNA or control shRNA were treated with proteosome inhibitor MG132. Ubiquitination of cortactin were determined by immunoblotting of ubiquitin following Flag-tag immunoprecipitation.

dependent manner (Fig. 4D). To further assess the effects of $Ca_v2.2$ on cortactin stability, we added cycloheximide (CHX) which suppresses protein synthesis and monitor the degradation of cortactin protein. As shown in Fig. 4E, cortactin stability was dramatically decreased in $Ca_v2.2$ knock-down cells. These results demonstrated that $Ca_v2.2$ stabilizes cortactin in breast cancer cells. We next examined whether $Ca_v2.2$ regulated cortactin ubiquitination or deubiquitination in breast cancer cells. As shown in Fig. 4F, knock-down of $Ca_v2.2$ in MDA-MB-231 cells strongly increased the ubiquitination of cortactin. These data demonstrated that $Ca_v2.2$ modulated the protein stability of cortactin through ubiquitination or deubiquitination process in breast cancer cells.

Identification of USP43 as a deubiquitinating enzyme for cortactin stability

As $Ca_v2.2$ is a calcium channel protein located on the cell surface, it is unlikely that it directly deubiquitinates cortactin. To gain insight how $Ca_v2.2$ decreased cortactin ubiquitination, we analyzed the correlation between the expression of cortactin and ubiquitin ligases or deubiquinating enzymes by using the proteomics data from Cancer Cell Line Encyclopedia (CCLE) database. Candidates from the analysis should satisfy the following criteria: (1) p value and q value below 0.01; (2) the Pearson correlation coefficient above zero if the candidate is a deubiquitinase. Conversely, Pearson correlation coefficient below zero if the candidate is a E3 ligase. Only six deubiquitinating enzymes (DUBs), USP43, OTUD1, OTUD4, OTUD7A, USP40, USP54 met our criteria. We then transfected the cDNAs of these six DUBs into MDA-MB-231 cells, and immunoblotting showed that only USP43 increased cortactin expression (Supplementary Fig. 9A). The expressions of these six DUBs were confirmed by real-time PCR (Supplementary Fig. 9B–G). We first determined whether USP43 interacted with cortactin. Immunoprecipitation showed that USP43 interacted with cortactin in MDA-MB-231 cells (Fig. 5A). Knock-down of USP43 in MDA-MB-231 cells decreased the expression of cortactin at the protein level (Fig. 5B) but did not affect its transcript (Fig. 5C). Conversely, over-expression of USP43 increased cortactin protein expression without affecting its expression at the transcriptional level (Fig. 5D, E). The addition of MG132 successfully rescued the decrease of cortactin expression caused by USP43 knock-down (Fig. 5F), while the addition of CHX resulted in more unstable cortactin protein in USP43 knock-down cells (Fig. 5G). These results demonstrated that USP43 stabilized cortactin protein in MDA-MB-231 cells. We next investigated whether USP43 was able to modulate cortactin ubiquitination in MDA-MB-231 cells. Knock-down of USP43 increased the addition of ubiquitin on cortactin (Fig. 5H). Together, these results suggested that USP43 directly regulates cortactin stability through deubiquitination.

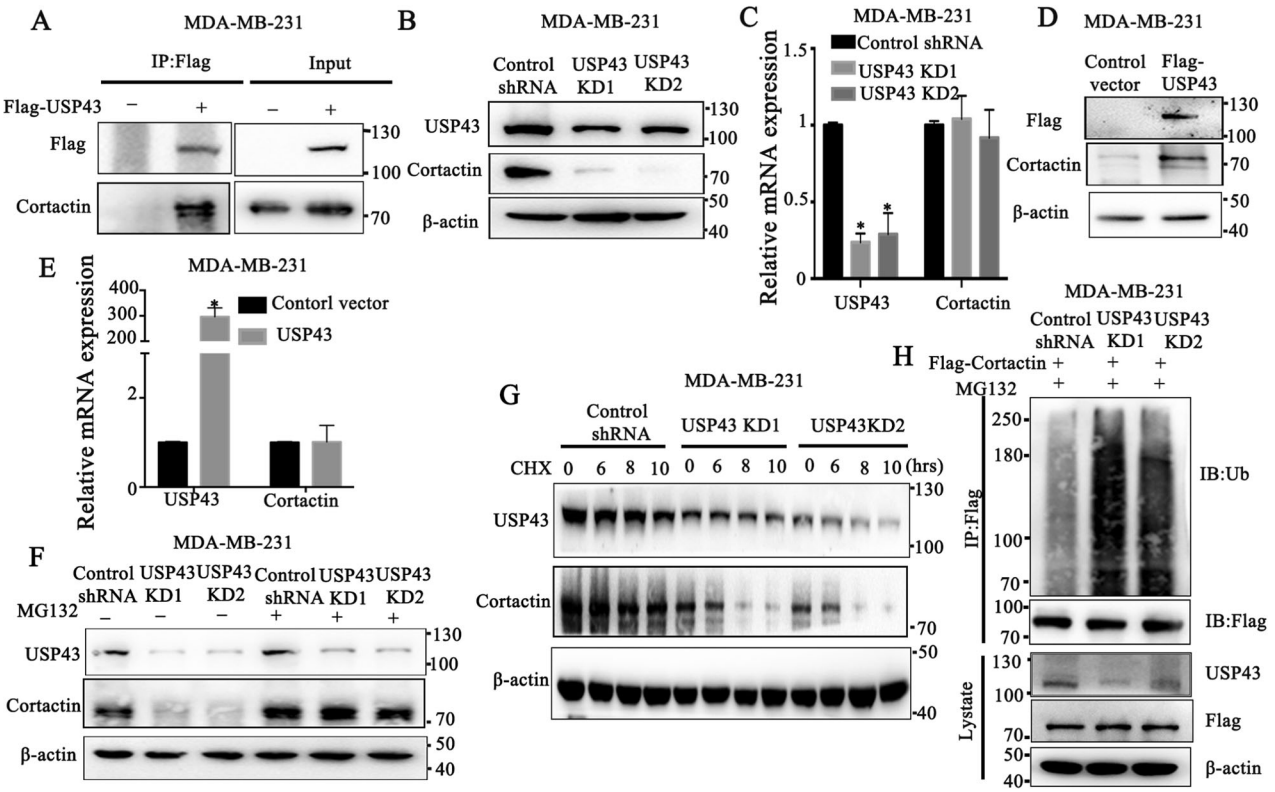

Fig. 5 USP43 interacts with and deubiquitinates cortactin. A Cortactin were determined by immunoblotting in MDA-MB-231 cells expressing Flag-tagged USP43 or control vector following Flag-tag immunoprecipitation. **B** Cortactin were determined by immunoblotting in MDA-MB-231 cells expressing USP43 shRNA or control shRNA. **C** Cortactin and USP43 transcripts were determined by qRT-PCR in MDA-MB-231 cells expressing USP43 shRNA or control shRNA. P value was determined using Student's t-test (*$p < 0.001$). Error bars represent mean ± s.d. **D** Cortactin were determined by immunoblotting in MDA-MB-231 cells expressing flag-tagged USP43 cDNA or a control vector. **E** Cortactin and USP43 transcripts were determined by qRT-PCR in MDA-MB-231 cells expressing USP43 cDNA or a control vector. **F** Cortactin and USP43 were determined by immunoblotting in MDA-MB-231 cells stably expressing USP43 shRNA or control shRNA and treated with proteosome inhibitor MG132 or a control vehicle. **G** Cortactin and USP43 were determined by immunoblotting in MDA-MB-231 cells stably expressing USP43 shRNA or control shRNA and treated with protein synthesis inhibitor cycloheximide (CHX) or a control vehicle. **H** MDA-MB-231 cells stably expressing Flag-tagged cortactin and USP43 shRNA or control shRNA were treated with proteosome inhibitor MG132. Ubiquitination of cortactin determined by immunoblotting of ubiquitin following Flag-tag immunoprecipitation.

USP43 mediates the functions of $Ca_v2.2$ in cortactin stabilization, invadopodia formation, and metastasis in breast cancer

To determine whether USP43 mediated the functions of $Ca_v2.2$, we introduced $Ca_v2.2$ shRNA and USP43 cDNA constructs into breast cancer cells. Immunoblotting showed that cortactin expression was stabilized in $Ca_v2.2$ knock-down cells expressing USP43 (Fig. 6A), indicating USP43 mediated the function of $Ca_v2.2$ in cortactin stabilization. We further investigated whether USP43 mediated $Ca_v2.2$ function in invadopodia formation, we expressed USP43 cDNA in $Ca_v2.2$ knock-down cells and found that USP43 expression rescued the decrease of invadopodia formation caused by $Ca_v2.2$ knock-down (Fig. 6B, C). Similarly, focal matrix degradation was also rescued in USP43 cDNA expression cells (Fig. 6D, E). To further investigate if USP43 mediated the function of $Ca_v2.2$ in metastasis in vivo, we transplanted luciferase-tagged MDA-MB-436 cells stably expressing $Ca_v2.2$ shRNA and USP43 cDNA constructs into mice. Seven out of ten mice transplanted with cells expressing $Ca_v2.2$ shRNA and USP43 developed metastases, whereas two out of ten mice expressing $Ca_v2.2$ shRNA developed metastasis (Fig. 6F). The luciferase signal of metastasis was also significantly higher in mice injected with cells expressing $Ca_v2.2$ shRNA and USP43 (Fig. 6F). These results indicated that USP43 mediated the functions of $Ca_v2.2$ in cortactin expression, invadopodia formation, ECM degradation, and metastasis.

USP43 is directly regulated by NFAT2

We then investigated the regulation of USP43 by $Ca_v2.2$ and found that knock-down of $Ca_v2.2$ decreased USP43 expression whereas over-expression of $Ca_v2.2$ increased USP43 expression transcriptionally and at the protein level (Fig. 7A–C). These results showed that $Ca_v2.2$ is sufficient and required for USP43 expression. We further explored the molecular mechanism of this regulation. Because $Ca_v2.2$ is a calcium channel, we first tested whether $[Ca^{2+}]$i (intracellular calcium level) was changed upon the decrease or increase of $Ca_v2.2$ expression. $[Ca^{2+}]$i was significantly decreased in $Ca_v2.2$ knock-down cells (Supplementary Fig. 10). Conversely, $[Ca^{2+}]$i level was significantly elevated in $Ca_v2.2$ overexpression cells (Supplementary Fig. 10). These results confirmed that $Ca_v2.2$ regulates calcium influx. Calcium influx activates heterodimeric phosphatase calcineurin, which dephosphorylates NFAT family proteins (NFAT1, NFAT2, NFAT3, NFAT4) andresults in their nuclear translocation [46]. Nuclear NFAT family proteins activate target gene expression, thus directly linking calcium signaling to gene expression [46]. We then investigated whether NFAT proteins were able to modulate USP43 mRNA expression. We found that depletion of NFAT2 and NFAT3 could significantly reduced USP43 mRNA expression (Fig. 7D, Supplementary Fig. 11). However, the knock-down of NFAT1 and NFAT4 did not decrease USP43 mRNA expression (Supplementary Fig. 12). We further determined the USP43 protein expression in NFAT2 or NFAT3 knock-down cells. NFAT2 or NFAT3 knock-down resulted in the decrease of USP43

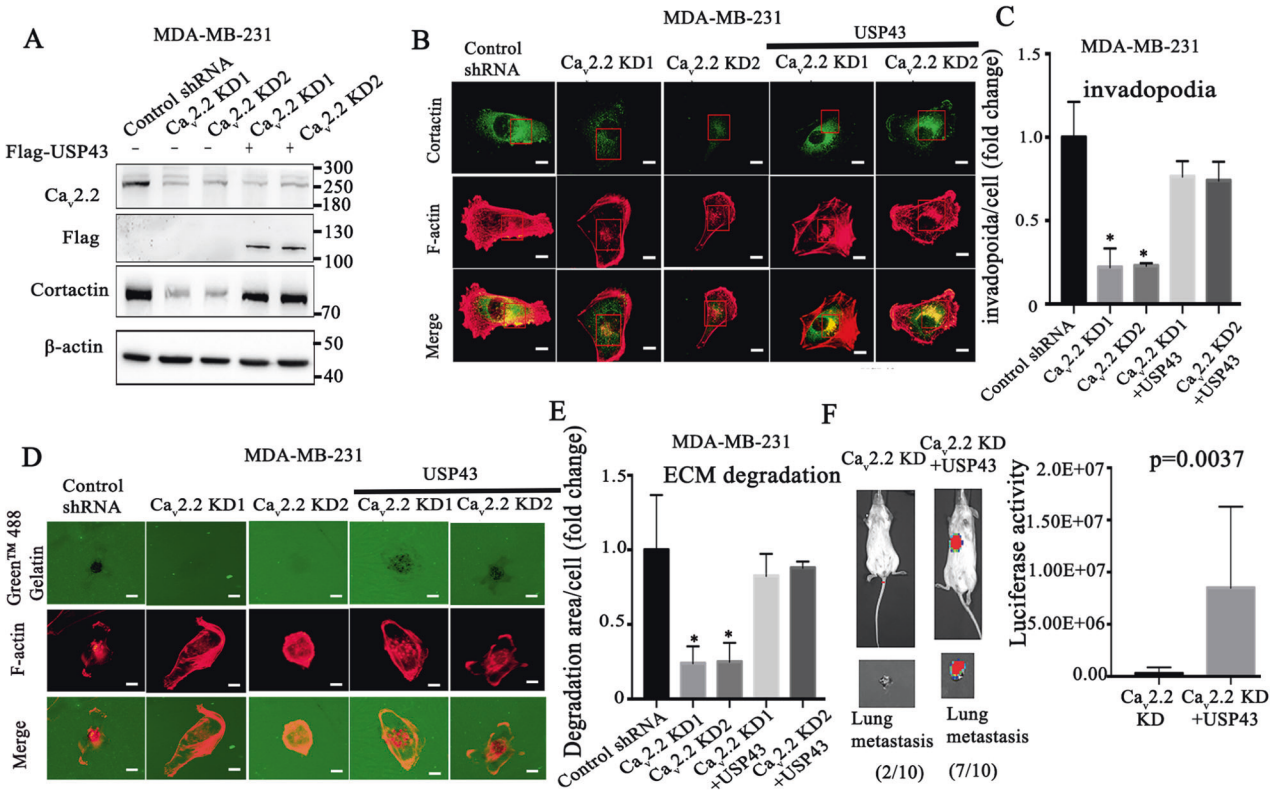

Fig. 6 USP43 mediates the function of Cav2.2 in cortactin stabilization, invadopodia formation, ECM degradation and metastasis in breast cancer. A $Ca_v2.2$ and cortactin were determined by immunoblotting in MDA-MB-231 cells expressing Flag-tagged USP43 and $Ca_v2.2$ shRNA or control shRNA. **B** MDA-MB-231 expressing USP43 cDNA and $Ca_v2.2$ shRNA or control shRNA were subjected to invadopodia formation assay. Invadopodia were visualized by co-localization of cortactin (green) and F-actin puncta (red). Representative images were shown. Bars: 5 μm. **C** Quantification of invadopodia in MDA-MB-231 cells. *P* value was determined using Student's t-test (*$p < 0.01$). Error bars represent mean ± s.d. **D** MDA-MB-231 cells expressing USP43 cDNA and $Ca_v2.2$ shRNAs or control shRNA were subjected to ECM degradation assay. Focal matrix degradation was defined by co-localization of F-actin and degradation regions. Representative images were shown. Bars: 5 μm. **E** Quantification of ECM degradation in MDA-MB-231 cells. *P* value was determined using Student's t-test (*$p < 0.01$). Error bars represent mean ± s.d. **F** Luciferase-tagged human breast cancer MDA-MB-436 cells stably expressing Cav2.2 shRNA or Cav2.2 shRNA and USP43 cDNA were transplanted in mice. Luciferase signal of metastasis was quantified using Xenogen bioluminescence system. *P* value was determined using Fisher's exact test ($p = 0.0037$).

protein expression (Fig. 7E, Supplementary Fig. 13). The ChIP analysis showed that NFAT3 did not bind to the NFAT consensus sequence in the USP43 promoter region we studied, but binded to the BACE1 promoter region which is a well-established direct target gene of NFAT3 and served as a control [47] (Supplementary Fig. 14A, Supplementary Fig. 14B). It is possible that NFAT3 binds to the other regions of USP43 promoter or indirectly regulates USP43 expression. Since we intend to find a transcription factor that directly regulates USP43 expression, we chose to focus on NFAT2 for further study. We transduced NFAT2 cDNA into MDA-MB-231 cells. Expression of NFAT2 increased USP43 mRNA and protein expression (Fig. 7F, G). These results suggested that USP43 is regulated by NFAT2. To determine whether USP43 is a direct target of NFAT2, we found two consensus binding sites (ggaaa) of NFAT2 in the USP43 promoter region (Fig. 7H) [48]. To verify whether USP43 is directly regulated by NFAT2, we cloned USP43 promoter (−213~−1847bp) into pGL3-basic vector and performed dual luciferase reporter assay. NFAT2 expression significantly increased the luciferase signal driven by the USP43 promoter (Fig. 7H). We used Chromatin Immunoprecipitation (ChIP) analysis to further determined the direct interactions of NFAT2 with USP43 promoter in MDA-MB-231 cells, ChIP analysis indicated the significant enrichment of USP43 promoter as well as BMI1 promoter which is a well-established direct target gene of NFAT2 [49] and served as a control in NFAT2 immunoprecipitation (Fig. 7I, Supplementary Fig. 15). These data suggested that NFAT2 directly regulates USP43 transcription.

$Ca_v2.2$ regulates USP43 expression through NFAT2 dephosphorylation

We further investigated whether NFAT2 mediates the function of $Ca_v2.2$ in USP43 regulation. We knocked down NFAT2 expression in $Ca_v2.2$ over-expression cells and determined USP43 expressions. NFAT2 knock-down abolished the up-regulation of USP43 levels by $Ca_v2.2$ (Fig. 8A, B). These data indicated that NFAT2 mediates the regulation of USP43 by $Ca_v2.2$. We next determined the molecular mechanism of NFAT regulation by $Ca_v2.2$. $Ca_v2.2$ knockdown increased the phosphorylation of NFAT2 and its cytoplasmic localization, while decreased NFAT2 nuclear localization. (Fig. 8C–E). Together, these experiments suggested that $Ca_v2.2$ is required for the direct regulation of USP43 by NFAT2.

DISCUSSION

The functions of calcium channels in tumor metastasis are poorly understood. Our study identified the role of calcium channel $Ca_v2.2$ in breast cancer metastasis and its underlying mechanism (Fig. 9). $Ca_v2.2$ was required for metastasis by promoting invadopodia formation. Surprisingly deubiquinating enzyme USP43 mediated the function of $Ca_v2.2$ in invadopodia formation

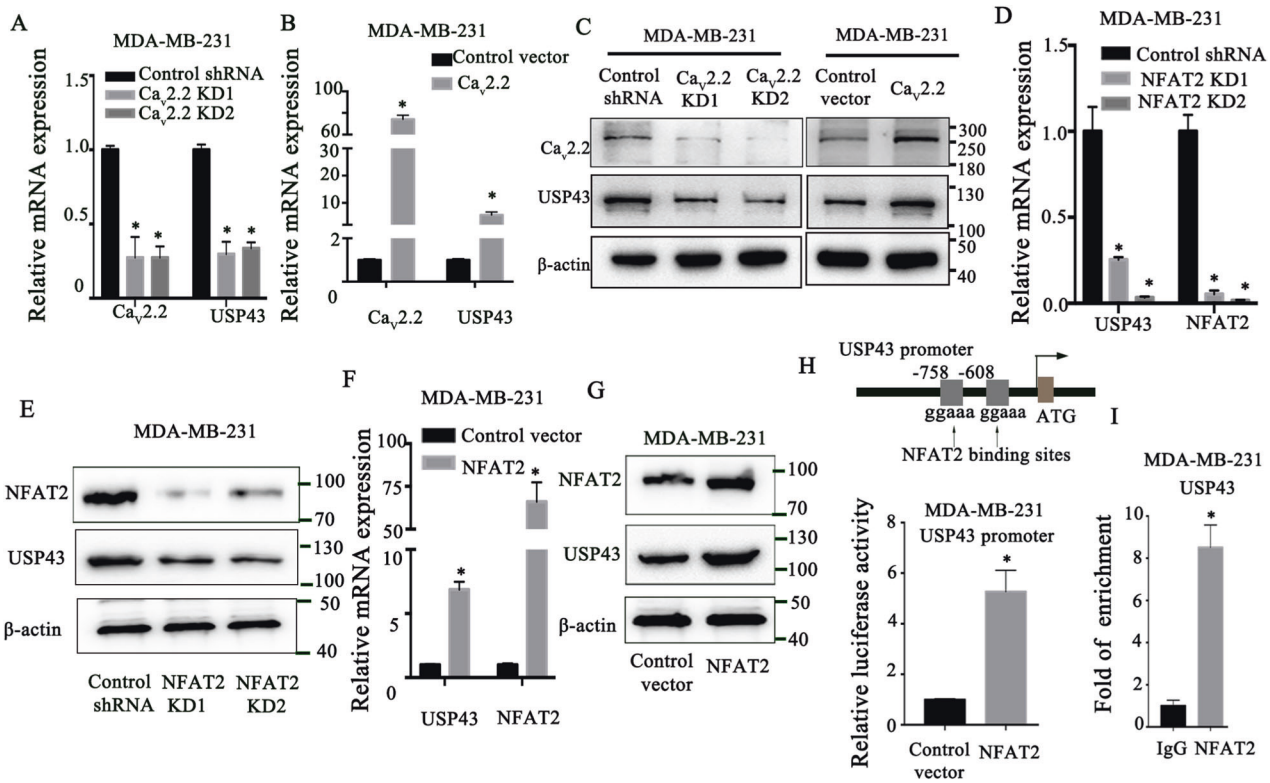

Fig. 7 USP43 is directly regulated by NFAT2. A $Ca_v2.2$ and USP43 expression were determined by qRT-PCR in MDA-MB-231 cells stably expressing $Ca_v2.2$ shRNA or a control shRNA. P value (*$p < 0.001$) was determined using Student's t-test. Error bars represent mean ± s.d. **B** $Ca_v2.2$ and USP43 expression were determined by qRT-PCR in MDA-MB-231 cells expressing $Ca_v2.2$ cDNA or a control vector. **C** USP43 and $Ca_v2.2$ expression were determined by immunoblotting in MDA-MB-231 cells stably expressing $Ca_v2.2$ shRNA or a control shRNA, $Ca_v2.2$ cDNA or a control vector. **D** USP43 and NFAT2 expression were determined by qRT-PCR in MDA-MB-231 cells expressing NFAT2 shRNA or a control shRNA. P value (*$p < 0.001$) was determined using Student's t-test. Error bars represent mean ± s.d. **E** NFAT2 and USP43 expression were determined by immunoblotting in MDA-MB-231 cells stably expressing NFAT2 shRNA or a control shRNA. **F** USP43 and NFAT2 expression were determined by qRT-PCR in MDA-MB-231 cells expressing NFAT2 cDNA or a control vector. P value (*$p < 0.001$) was determined using Student's t-test. Error bars represent mean ± s.d. **G** NFAT2 and USP43 expression were determined by immunoblotting in MDA-MB-231 cells stably expressing NFAT2 cDNA or a control vector. **H** NFAT2 binding sites on the USP43 promoter were showned (top). The luciferase activity of USP43-promoter was determined by dual lucifierase reporter assay in MDA-MB-231 cells expressing pGL3-USP43 promoter-Luc plasimid and NFAT2 cDNA or a control vector (bottom). Luciferase activity values were normalized to renilla luciferase activity values and expressed as fold change over a control vector. P value (*$p < 0.001$) was determined using Student's t-test. Error bars represent mean ± s.d. **I** Chromatin immunoprecipitation (ChIP) was performed using an anti-NFAT2 antibody or a control IgG. The USP43 promoter region where NFAT2 binds showed significant enrichment after immunoprecipitation by an anti-NFAT2 antibody. *P* value (*$p < 0.001$) was determined using Student's t-test. Error bars represent mean ± s.d.

by stabilizing cortactin, a critical component of invadopodia. Strikingly, $Ca_v2.2$ regulates USP43 mRNA and protein levels by activating calcineurin/NFAT2 signaling. To our knowledge, this is the first time calcium channel $Ca_v2.2$ and deubiquitination process have been shown to play roles in invadopodia formation. Our study also revealed the functions of deubiquitinase USP43 in breast cancer cell migration, invasion, and metastasis. These studies uncovered a novel pathway that regulated invadopodia formation and metastasis in breast cancer.

$Ca_v2.2$ is exclusively expressed in neuronal tissues but not in breast epithelial cells. The expression of a tissue-specific gene in the cancer of another tissue type presents a unique opportunity for therapy development. For an example, neuronal-specific glutamate receptor GRM1 is aberrantly expressed in melanoma and has been shown to play a critical role in melanoma development. GRM1 inhibitors as therapies for melanoma are currently in clinical trials. Ziconotide is an FDA-approved $Ca_v2.2$ blocker for the treatment of severe and chronic pain. It is worthwhile to determine if ziconotide and other N-type calcium channel blockers can be used as therapies for the treatment of breast cancer metastasis. Development of novel $Ca_v2.2$ blockers that are not able to cross blood–brain barrier may be even better for the treatment of breast cancer metastasis.

Invadopodia formation is required for breast cancer cells to degrade extracellular matrix and invade neighboring tissues [50]. However, invadopodia is difficult to target for therapy development because the main components of invadopodia F-actin and actin regulatory proteins are structurally undruggable. Our finding that deubiquiting enzyme USP43 regulates invadopodia formation may present a novel therapeutic target for the suppression of invadopodia and metastasis.

Our studies opened up a number of questions regarding the roles of $Ca_v2.2$, NFAT2 and USP43 in invadopodia formation and metastasis. USP43 functions as a deubiquitinase. We have shown that cortactin is a substrate of USP43 in this study. Whether other factors in metastasis are also substrates of USP43 is unknown. The identification of substrates of USP43 that regulate invadopodia formation and metastatic process will improve our knowledge of the roles of ubiquiting process in metastasis. Cortactin regulation is also complex. In addition to the deubiquitination process we identified, it has been shown that phosphorylation can also regulate cortactin activity [36, 51]. The elucidation of the interplay

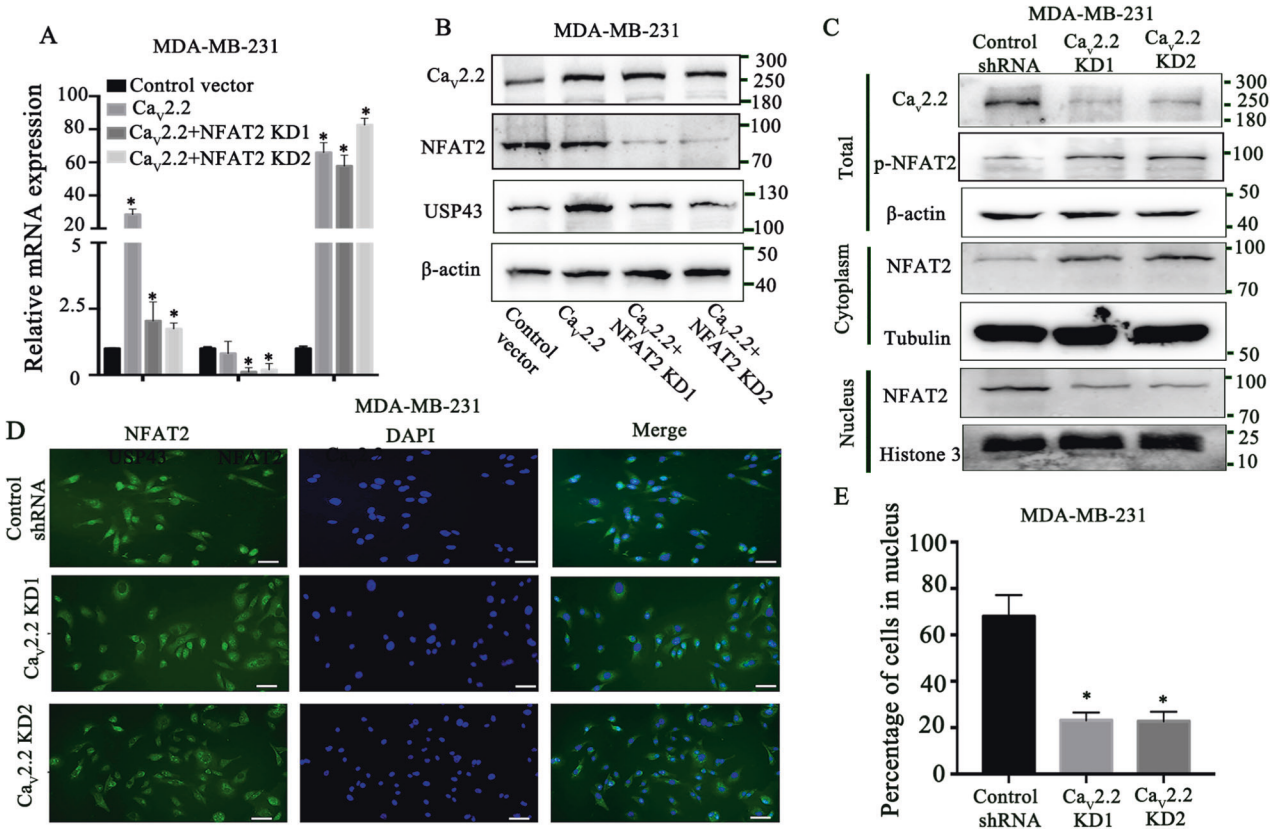

Fig. 8 Cav2.2 regulates USP43 expression through NFAT2 dephosphorylation. A USP43, NFAT2, and $Ca_v2.2$ expression were determined by qRT-PCR in MDA-MB-231 cells expressing $Ca_v2.2$ cDNA and NFAT2 shRNA or a control shRNA. P value was determined using Student's t-test (*$p < 0.001$). Error bars represent mean ± s.d. **B** $Ca_v2.2$, NFAT2, and USP43 expression were determined by immunoblotting in MDA-MB-231 cells expressing $Ca_v2.2$ cDNA and NFAT2 shRNA or a control shRNA. **C** $Ca_v2.2$ and phosphorylated NFAT2 expression were determined by immunoblotting in MDA-MB-231 cells expressing $Ca_v2.2$ shRNA or a control shRNA. NFAT2 expression in cyltoplasm and nucleus were determined by immunoblotting in MDA-MB-231 cells expressing $Ca_v2.2$ shRNA or a control shRNA. **D** The subcellular localization of NFAT2 was determined by immunofluorescence in MDA-MB-231 cells expressing $Ca_v2.2$ shRNA or a control shRNA. Representative images were shown. Bars: 20 μm. **E** Quantification of NFAT2 nuclear abundance in MDA-MB-231 cells expressing $Ca_v2.2$ shRNA or a control shRNA. *P* value was determined using Student's t-test (*$p < 0.01$). Error bars represent mean ± s.d.

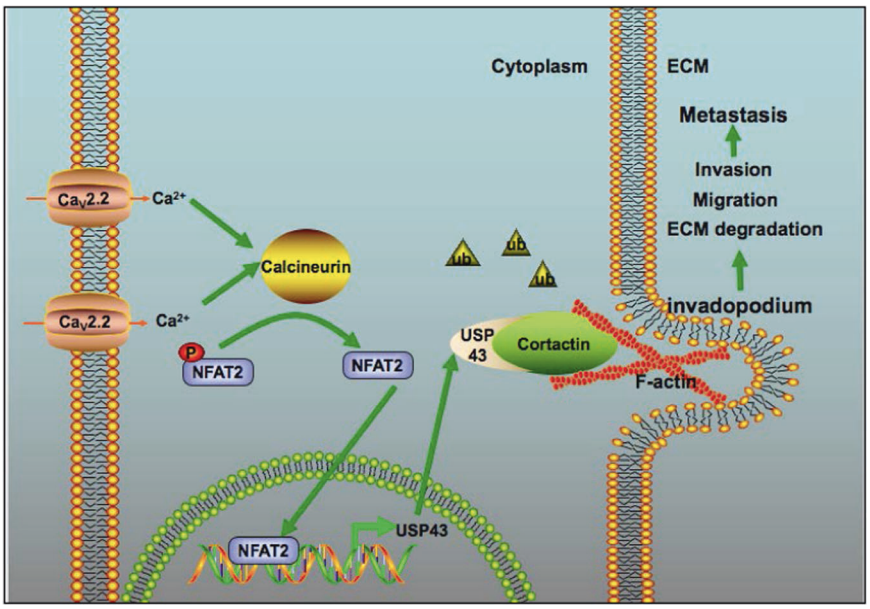

Fig. 9 The working model of deubiquitinase USP43 mediating the functions of the calcium channel Cav2.2 in cortactin stabilization, invadopodia formation, and metastasis. $Ca_v2.2$ up-regulates USP43 expression through NFAT2 dephosphorylation and nuclear localization. USP43 stablizes cortactin through deubiquitination and promotes invadopodia formation and metastasis.

between these regulatory processes in invasive cancer cells is critical to the understanding of tumor invasion and metastasis.

DATA AVAILABILITY

The data supporting the findings of this study are available within the article and its supplementary information files.

REFERENCES

1. Siegel RL, Miller KD, Jemal A. Cancer statistics, 2020. CA: Cancer J Clin. 2020;70:7–30.
2. Nanou E, Catterall WA. Calcium channels, synaptic plasticity, and neuropsychiatric disease. Neuron 2018;98:466–81.
3. Dolphin AC. Calcium channel auxiliary α2δ and β subunits: trafficking and one step beyond. Nat Rev Neurosci. 2012;13:542–55.
4. Williams ME, Brust PF, Feldman DH, Patthi S, Simerson S, Maroufi A, et al. Structure and functional expression of an omega-conotoxin-sensitive human N-type calcium channel. Sci (N. Y, NY). 1992;257:389–95.
5. Heinke B, Balzer E, Sandkühler J. Pre- and postsynaptic contributions of voltage-dependent Ca2+ channels to nociceptive transmission in rat spinal lamina I neurons. Eur J Neurosci. 2004;19:103–11.
6. Matthews EA, Dickenson AH. Effects of spinally delivered N- and P-type voltage-dependent calcium channel antagonists on dorsal horn neuronal responses in a rat model of neuropathy. Pain 2001;92:235–46.
7. Winquist RJ, Pan JQ, Gribkoff VK. Use-dependent blockade of Cav2.2 voltage-gated calcium channels for neuropathic pain. Biochem Pharmacol. 2005;70:489–99.
8. Wall MJ, Subasinghe NL, Winters MP, Lubin ML, Finley MFA, Qin N, et al. Discovery and optimization of a novel series of pyrazolyltetrahydropyran N-type calcium channel (Ca(v) 2.2) blockers for the treatment of pain. Bioorg Med Chem Lett. 2018;28:3780–3.
9. Simms BA, Zamponi GW. Neuronal voltage-gated calcium channels: structure, function, and dysfunction. Neuron 2014;82:24–45.
10. Komuro H, Rakic P. Selective role of N-type calcium channels in neuronal migration. Sci (N. Y, NY). 1992;257:806–9.
11. Gorman KM, Meyer E, Grozeva D, Spinelli E, McTague A, Sanchis-Juan A, et al. Bi-allelic loss-of-function CACNA1B mutations in progressive epilepsy-dyskinesia. Am J Hum Genet. 2019;104:948–56.
12. Chiang AC, Massagué J. Molecular basis of metastasis. N. Engl J Med. 2008;359:2814–23.
13. Kessenbrock K, Plaks V, Werb Z. Matrix metalloproteinases: regulators of the tumor microenvironment. Cell 2010;141:52–67.
14. Yamaguchi H, Lorenz M, Kempiak S, Sarmiento C, Coniglio S, Symons M, et al. Molecular mechanisms of invadopodium formation: the role of the N-WASP-Arp2/3 complex pathway and cofilin. J Cell Biol. 2005;168:441–52.
15. Chen WT. Proteolytic activity of specialized surface protrusions formed at rosette contact sites of transformed cells. J Exp Zool. 1989;251:167–85.
16. Leong HS, Robertson AE, Stoletov K, Leith SJ, Chin CA, Chien AE, et al. Invadopodia are required for cancer cell extravasation and are a therapeutic target for metastasis. Cell Rep. 2014;8:1558–70.
17. Eckert MA, Lwin TM, Chang AT, Kim J, Danis E, Ohno-Machado L, et al. Twist1-induced invadopodia formation promotes tumor metastasis. Cancer Cell. 2011;19:372–86.
18. Marx J. Cell biology. Podosomes and invadopodia help mobile cells step lively. Sci (N. Y, NY). 2006;312:1868–9.
19. Beaty BT, Condeelis J. Digging a little deeper: the stages of invadopodium formation and maturation. Eur J Cell Biol. 2014;93:438–44.
20. Sibony-Benyamini H, Gil-Henn H. Invadopodia: the leading force. Eur J Cell Biol. 2012;91:896–901.
21. Weaver AM. Invadopodia: specialized cell structures for cancer invasion. Clin Exp Metastasis. 2006;23:97–105.
22. Eddy RJ, Weidmann MD, Sharma VP, Condeelis JS. Tumor cell invadopodia: invasive protrusions that orchestrate metastasis. Trends Cell Biol. 2017;27:595–607.
23. Hill A, McFarlane S, Mulligan K, Gillespie H, Draffin JE, Trimble A, et al. Cortactin underpins CD44-promoted invasion and adhesion of breast cancer cells to bone marrow endothelial cells. Oncogene 2006;25:6079–91.
24. Clark ES, Whigham AS, Yarbrough WG, Weaver AM. Cortactin is an essential regulator of matrix metalloproteinase secretion and extracellular matrix degradation in invadopodia. Cancer Res. 2007;67:4227–35.
25. Uruno T, Liu J, Zhang P, Fan Y, Egile C, Li R, et al. Activation of Arp2/3 complex-mediated actin polymerization by cortactin. Nat Cell Biol. 2001;3:259–66.
26. Weaver AM, Heuser JE, Karginov AV, Lee WL, Parsons JT, Cooper JA. Interaction of cortactin and N-WASp with Arp2/3 complex. Curr Biol. 2002;12:1270–8.
27. Artym VV, Zhang Y, Seillier-Moiseiwitsch F, Yamada KM, Mueller SC. Dynamic interactions of cortactin and membrane type 1 matrix metalloproteinase at invadopodia: defining the stages of invadopodia formation and function. Cancer Res. 2006;66:3034–43.
28. Tehrani S, Tomasevic N, Weed S, Sakowicz R, Cooper JA. Src phosphorylation of cortactin enhances actin assembly. Proc Natl Acad Sci USA. 2007;104:11933–8.
29. Chánez-Paredes S, Montoya-García A, Castro-Ochoa KF, García-Cordero J, Cedillo-Barrón L, Shibayama M, et al. The Arp2/3 inhibitory protein arpin is required for intestinal epithelial barrier integrity. Front Cell Dev Biol. 2021;9:625719.
30. Cai L, Makhov AM, Schafer DA, Bear JE. Coronin 1B antagonizes cortactin and remodels Arp2/3-containing actin branches in lamellipodia. Cell 2008;134:828–42.
31. Zhao G, Zhang H, Huang Z, Lv L, Yan F. Cortactin and Exo70 mediated invasion of hepatoma carcinoma cells by MMP-9 secretion. Mol Biol Rep. 2016;43:407–14.
32. Lua BL, Low BC. Cortactin phosphorylation as a switch for actin cytoskeletal network and cell dynamics control. FEBS Lett. 2005;579:577–85.
33. Martinez-Quiles N, Ho HY, Kirschner MW, Ramesh N, Geha RS. Erk/Src phosphorylation of cortactin acts as a switch on-switch off mechanism that controls its ability to activate N-WASP. Mol Cell Biol. 2004;24:5269–80.
34. Oser M, Mader CC, Gil-Henn H, Magalhaes M, Bravo-Cordero JJ, Koleske AJ, et al. Specific tyrosine phosphorylation sites on cortactin regulate Nck1-dependent actin polymerization in invadopodia. J Cell Sci. 2010;123:3662–73. Pt 21
35. Vistein R, Puthenveedu MA. Src regulates sequence-dependent beta-2 adrenergic receptor recycling via cortactin phosphorylation. Traffic (Cph, Den). 2014;15:1195–205.
36. Schnoor M, Stradal TE, Rottner K. Cortactin: cell functions of a multifaceted actin-binding protein. Trends Cell Biol. 2018;28:79–98.
37. Gumireddy K, Li A, Yan J, Setoyama T, Johannes GJ, Orom UA, et al. Identification of a long non-coding RNA-associated RNP complex regulating metastasis at the translational step. EMBO J. 2013;32:2672–84.
38. Gumireddy K, Li A, Kossenkov AV, Sakurai M, Yan J, Li Y, et al. The mRNA-edited form of GABRA3 suppresses GABRA3-mediated Akt activation and breast cancer metastasis. Nat Commun. 2016;7:10715.
39. Paz H, Pathak N, Yang J. Invading one step at a time: the role of invadopodia in tumor metastasis. Oncogene 2014;33:4193–202.
40. Bowden ET, Onikoyi E, Slack R, Myoui A, Yoneda T, Yamada KM, et al. Co-localization of cortactin and phosphotyrosine identifies active invadopodia in human breast cancer cells. Exp Cell Res. 2006;312:1240–53.
41. Murphy DA, Courtneidge SA. The 'ins' and 'outs' of podosomes and invadopodia: characteristics, formation and function. Nat Rev Mol Cell Biol. 2011;12:413–26.
42. Ridley AJ. Life at the leading edge. Cell 2011;145:1012–22.
43. Nürnberg A, Kitzing T, Grosse R. Nucleating actin for invasion. Nat Rev Cancer. 2011;11:177–87.
44. Dikic I, Wakatsuki S, Walters KJ. Ubiquitin-binding domains - from structures to functions. Nat Rev Mol Cell Biol. 2009;10:659–71.
45. Shcherbik N, Haines DS. Ub on the move. J Cell Biochem. 2004;93:11–9.
46. Shibasaki F, Price ER, Milan D, McKeon F. Role of kinases and the phosphatase calcineurin in the nuclear shuttling of transcription factor NF-AT4. Nature 1996;382:370–3.
47. Mei Z, Yan P, Tan X, Zheng S, Situ B. Transcriptional regulation of BACE1 by NFAT3 leads to enhanced amyloidogenic processing. Neurochem Res. 2015;40:829–36.
48. Macián F, López-Rodríguez C, Rao A. Partners in transcription: NFAT and AP-1. Oncogene 2001;20:2476–89.
49. Wu L, Zhang D, Zhou L, Pei Y, Zhuang Y, Cui W, et al. FUN14 domain-containing 1 promotes breast cancer proliferation and migration by activating calcium-NFATC1-BMI1 axis. EBioMedicine 2019;41:384–94.
50. Meirson T, Gil-Henn H. Targeting invadopodia for blocking breast cancer metastasis. Drug resistance updates: Rev commentaries antimicrobial anticancer Chemother. 2018;39:1–17.
51. Zhao J, Wei J, Mialki R, Zou C, Mallampalli RK, Zhao Y. Extracellular signal-regulated kinase (ERK) regulates cortactin ubiquitination and degradation in lung epithelial cells. J Biol Chem. 2012;287:19105–14.

ACKNOWLEDGEMENTS

This study was supported by Ministry of Science and Technology of China (2021YFA0804700) (QH), National Natural Science Foundation of China (82072914 and 81872358) (QH), National Key Research and Development Program of China (2020YFC2008400) (C.M.)

AUTHOR CONTRIBUTIONS

QH and XZ conceived and designed the experiments as well as wrote the manuscript; YX and ML performed experiments, analyzed and interpreted data; JH, YS, WG, CM and DG discussed the experiments. YH, XW, XH and TL reviewed and edited the manuscript. All authors read and approved the final manuscript.

CONFLICT OF INTEREST

The authors declare no competing interests.

ADDITIONAL INFORMATION

Supplementary information The online version contains supplementary material available at https://doi.org/10.1038/s41419-022-05174-0.

Correspondence and requests for materials should be addressed to Xiaoping Zhang or Qihong Huang.

Reprints and permission information is available at http://www.nature.com/reprints

Publisher's note Springer Nature remains neutral with regard to jurisdictional claims in published maps and institutional affiliations.

Open Access This article is licensed under a Creative Commons Attribution 4.0 International License, which permits use, sharing, adaptation, distribution and reproduction in any medium or format, as long as you give appropriate credit to the original author(s) and the source, provide a link to the Creative Commons license, and indicate if changes were made. The images or other third party material in this article are included in the article's Creative Commons license, unless indicated otherwise in a credit line to the material. If material is not included in the article's Creative Commons license and your intended use is not permitted by statutory regulation or exceeds the permitted use, you will need to obtain permission directly from the copyright holder. To view a copy of this license, visit http://creativecommons.org/licenses/by/4.0/.

© The Author(s) 2022